

## ACCRETION FLOW DYNAMICS OF MAXI J1659-152 FROM THE SPECTRAL EVOLUTION STUDY OF ITS 2010 OUTBURST USING THE TCAF SOLUTION

DIPAK DEBNATH<sup>1</sup>, ASLAM ALI MOLLA<sup>1</sup>, SANDIP K. CHAKRABARTI<sup>2,1</sup>, SANTANU MONDAL<sup>1</sup>

(Dated: Accepted: 10th Feb. 2015; Received: 8th Dec. 2014)

*Draft version August 30, 2018*

### ABSTRACT

Transient black hole candidates are interesting objects to study in X-rays as these sources show rapid evolutions in their spectral and temporal properties. In this paper, we study the spectral properties of the Galactic transient X-ray binary MAXI J1659-152 during its very first outburst after discovery with the archival data of RXTE Proportional Counter Array instruments. We make a detailed study of the evolution of accretion flow dynamics during its 2010 outburst through spectral analysis using the Chakrabarti-Titarchuk two-component advective flow (TCAF) model as an additive table model in XSPEC. Accretion flow parameters (Keplerian disk and sub-Keplerian halo rates, shock location and shock strength) are extracted from our spectral fits with TCAF. We studied variations of these fit parameters during the entire outburst as it passed through three spectral classes: *hard*, *hard-intermediate*, and *soft-intermediate*. We compared our TCAF fitted results with standard combined disk black body (DBB) and power-law (PL) model fitted results and found that variations of disk rate with DBB flux and halo rate with PL flux are generally similar in nature. There appears to be an absence of the soft state unlike what is seen in other similar sources.

*Subject headings:* X-Rays:binaries – stars individual: (MAXI J1659-152) – stars:black holes – accretion, accretion disks – shock waves – radiation:dynamics

### 1. INTRODUCTION

Compact objects, such as black holes (BHs) and neutron stars are identified by electromagnetic radiations emitted from the accreting disk formed by matter from their companion. This matter is accreted either through Roche-lobe overflow or winds. Some of these objects are transient stellar mass X-ray binaries with a low mass star acting as a donor star. Study of these objects in X-rays is very interesting as they undergo rapid evolution in their timing and spectral properties which are strongly correlated to each other. There are a large number of articles by several groups (see, e.g., McClintock & Remillard, 2006; Belloni et al. 2005; Nandi et al. 2012; Debnath et al. 2013, etc.) which discuss variation of spectral and temporal properties of these transient black hole candidates (BHCs) during their X-ray outbursts. In general, it has been found that these objects show different spectral states (hard, hard-intermediate, soft-intermediate, soft, etc.; McClintock & Remillard, 2006) and low and high frequency quasi-periodic oscillations (QPOs) in power-density spectra (PDS) in some of these spectral states (Remillard & McClintock, 2006). Different branches of X-ray color-color and Hardness-Intensity Diagrams (HIDs; Maccarone & Coppi, 2003; Belloni et al. 2005; Debnath et al. 2008, etc.) are related to different spectral states of the outburst phases. It has also been observed by several authors (see, Mandal & Chakrabarti, 2010; Nandi et al., 2012; Debnath et al., 2013 and references therein) that these observed spectral states show hysteresis loops during their spectral evolutions of an entire epoch of the outburst of these transient BHCs. Simple model fits of accretion rates using two component advective flow (TCAF) solution of

Chakrabarti-Titarchuk (1995, hereafter CT95) by Mandal and Chakrabarti (2010) indicated that indeed the accretion

rates vary differently in the rising and declining states.

In the literature, there are a large number of theoretical or phenomenological models, which describe accretion flow dynamics around a BH. It is well known that emitted radiation contains both thermal and non-thermal components. The thermal component is multi-color blackbody type emitted the standard Keplerian disk (Shakura & Sunyaev, 1973; Novikov & Thorne, 1973) and the other is a power-law component, originated from the so-called ‘Compton’ cloud (Sunyaev & Titarchuk, 1980; 1985). This component is composed of hot electrons and is cooled down by repeated Compton scatterings of the low energy (soft) photons. There are many speculations about the nature of this Compton cloud which range from it being a magnetic corona (Galeev, Rosner & Viana, 1979) to a hot gas corona over the disk (Haardt & Maraschi, 1991; Zdziarski et al., 2003). CT95, in their TCAF solution, considers that the CENTrifugal pressure supported BOUNDary Layer or CENBOL plays the role of the Compton cloud. This CENBOL happens to be the post-shock region of the low-angular momentum halo in which a standard Keplerian disk remains immersed while emitting soft photons. The shock in the halo forms due to the piling up of matter behind the centrifugal barrier of the low angular momentum accretion flow component having a sub-critical viscosity parameter (Chakrabarti 1990ab, hereafter C90ab, 1996). These shocks are found to be stable even under non-axisymmetric perturbations (Okuda, Teresi & Molteni, 2007). The other component of TCAF is an optically thick standard (SS73) Keplerian (disk) component which is formed in flows with super-critical viscosity parameter (C90ab). Of course, this disk also has to pass through the inner sonic point to satisfy the boundary conditions on the black hole horizon (C90ab; see also, Muchotrzeb & Paczyński, 1982). Formation of TCAF from a single simulation (see, Giri & Chakrabarti, 2013; Giri, Garain & Chakrabarti, 2015, and references therein) show that it has a stable configuration. Also, in Mondal et al. (2014a) a self-consistent transonic solution of TCAF in presence of both

dipak@csp.res.in; aslam@csp.res.in; chakraba@bose.res.in; santanu@csp.res.in

<sup>1</sup> Indian Center for Space Physics, 43 Chalanika, Garia St. Rd., Kolkata, 700084, India.

<sup>2</sup> S. N. Bose National Centre for Basic Sciences, Salt Lake, Kolkata, 700098, India.

cooling and outflows is obtained.

Recently, after the inclusion of this TCAF solution (CT95; Chakrabarti, 1997, hereafter C97) in HEASARC’s spectral analysis software package XSPEC as an additive table model Debnath, Chakrabarti & Mondal (2014, hereafter DCM14), Debnath, Mondal & Chakrabarti (2015, hereafter DMC15) and Mondal, Debnath & Chakrabarti (2014b, hereafter MDC14) obtained a clearer picture about the accretion flow dynamics around BHCs as they find evidences of systematically varying accretion rates of the standard disk and the halo and the shock location on a daily basis. From the TCAF fitted spectrum, one can obtain two accretion rates (disk and halo), shock locations and shock strength. These parameters also give us information about the frequency of QPOs. Transitions of various spectral states which are observed during the outburst phases of a transient BHC can be identified by special behaviour of accretion rate ratio (ARR) and the nature of observed QPOs.

Newly discovered MAXI J1659-152 is an interesting black hole binary to study because it is the shortest orbital period BHC observed till date (Kuulkers et al., 2010; 2013). The source was first observed by MAXI/GSC instrument on 25th Sept. 2010 at the sky location of R.A. =  $16^h59^m10^s$ , Dec =  $-15^\circ16'05''$  (Negoro et al., 2010). The source was simultaneously observed by SWIFT/BAT instrument roughly at  $17^\circ$  above the Galactic plane (Mangano et al. 2010). Kalamkar et al. (2011) defined the source as a BHC, based on their combined optical and X-ray spectral study, which was initially thought to be a Gamma-Ray Burst and was named as GRB100925A). Kuulkers et al. (2013) based on their detailed study of the X-ray intensity variation of observed absorption dips (Kennea et al. 2010), confirmed MAXI J1659-152 to be a short orbital period black hole binary of period =  $2.414 \pm 0.005$  hrs.

MAXI J1659-152 showed X-ray flaring activity in 2010, other than low-level activity in 2011 which continued for  $\sim 9$  months. During this period, the source was extensively studied in multi-wave band, such as various X-ray (Muñoz-Darias et al. 2011; Kalamkar et al. 2011; Yamaoka et al. 2012; Kuulkers et al. 2013), optical/IR (Russel et al. 2010; Kaur et al. 2012), and radio observatories (Miller-Jones et al. 2011; Paragi et al. 2013). van der Horst et al. (2013) made multi-band campaign to explore multi-wavelength properties of the source during this outburst. Physical parameters, such as distance, disk inclination angle, masses of the source and the companion are estimated using various methods. The most acceptable ranges of distance and disk inclination angle are 5.3 – 8.6 kpc and 60 – 80 degree (Yamaoka et al. 2012; Kuulkers et al. 2013) respectively. Although Shaposhnikov et al. (2011) predicted the mass of the BH ( $M_{BH}$ ) as  $20 \pm 3 M_\odot$ , the preferable range of mass of the source and companion are 3 – 8  $M_\odot$  (Yamaoka et al. 2012) and 0.15 – 0.25  $M_\odot$  (Kuulkers et al. 2013) respectively. In this paper, we use mass of the BH as 6  $M_\odot$ .

We study spectral and timing properties of the source during its 2010 main outburst phase, which continued for  $\sim 1.5$  months, using RXTE PCA archival data. Temporal properties of the BHC along with the evolution of QPO frequency during declining phase of the outburst are presented in Molla et al. (2015, hereafter Paper II).

The *paper* is organized in the following way: in the next Section, we briefly discuss observation and data analysis procedures using HEASARC’s HeaSoft software package. In §3, we present results of spectral analysis using TCAF *fits* file

as an additive table model in XSPEC and variation of different flow parameters extracted from model fits. Here, we also compare combined DBB and PL model fitted spectral analysis results with that of the TCAF fitted analysis results. Finally, in §4, we present a brief discussion and make our concluding remarks.

## 2. OBSERVATION AND DATA ANALYSIS

We analyze the data of 30 observational IDs starting from the first day of RXTE PCA observation, namely, 2010 September 28 (Modified Julian Day, i.e., MJD = 55467) to 2010 November 11 (MJD = 55508). Data reduction and analysis are done using HEASARC’s software package HeaSoft version HEADAS 6.15 and XSPEC version 12.8. To analyze archival data of the RXTE PCA instrument, we follow the standard data analysis techniques as done by Debnath et al. (2013, 2015).

For spectral analysis, *Standard2* mode Science Data of PCA (FS4a\*.gz) are used. Spectra are extracted from all the layers of the PCU2 for 128 channels (without any binning/grouping the channels). We exclude HEXTE data from our analysis, as we find strong residuals (line features) in the HEXTE spectra at different energies. This could be due to the fact that the ‘rocking’ mechanism for HEXTE stopped. So, we restrict our spectral analysis with the PCA data for the energy range of 2.5 – 25 keV only. In the entire PCA data analysis, we include the dead-time correction and also the PCA breakdown correction (because of the leakage of propane layers of PCUs). The “runpcabackest” task was used to estimate the PCA background using the latest bright-source background model. We also incorporated the *pca\_saa\_history* file to take care of the SAA data. To generate the response files, we used the “pcarsp” task. Detailed analysis will be discussed in Paper II.

The 2.5–25 keV PCA background subtracted spectra are fitted with TCAF based model *fits* file and with combined DBB and PL model components in XSPEC. Individual flux contributions for the DBB and PL model components are obtained by using the convolution model ‘cflux’ technique. For the entire outburst, we keep hydrogen column density ( $N_H$ ) fixed at  $3.0 \times 10^{21}$  atoms  $\text{cm}^{-2}$  (Muñoz-Darias et al., 2011) for absorption model *wabs*. We also assume a fixed 1.0% systematic instrumental error for the spectral study during entire phase of the outburst. After achieving the best fit based on reduced chi-square value ( $\chi_{red}^2 \sim 1$ ), ‘err’ command is used to find 90% confidence error values for the model fit parameters. In Appendix, Table I, we mention average values of these two errors in superscript.

For a spectral fit, using the TCAF based model, one needs to supply five model input parameters, other than the normalization constant. These parameters are: *i*) black hole mass ( $M_{BH}$ ) in solar mass ( $M_\odot$ ) unit, *ii*) sub-Keplerian rate ( $\dot{m}_h$  in  $\dot{M}_{Edd}$ ), *iii*) Keplerian rate ( $\dot{m}_d$  in Eddington rate  $\dot{M}_{Edd}$ ), *iv*) location of the shock ( $X_s$  in Schwarzschild radius  $r_g = 2GM/c^2$ ), *v*) compression ratio ( $R$ ) of the shock. The model normalization value (*norm*) is  $\frac{R_c^2}{4\pi D^2} \sin(i)$ , where ‘ $R_c^2$ ’ represents an effective area of the emitting region (purely on dimensional ground),  $D$  is the source distance in 10 kpc unit and  $i$  is the disk inclination angle. In order to fit a black hole spectrum with the TCAF model in XSPEC, we generate model *fits* file (*TCAF0.1.fits*) using theoretical spectra generating software by varying five input parameters in CT95 code. We then include it in XSPEC as a local additive model. A brief dis-

discussion of the TCAF model, its present development and a detailed description of the range of input parameters and generation procedure of the current version (v0.1) of the TCAF *fits* file are given in DCM14 and DMC15. For the spectral analysis with TCAF, mass of the black hole is frozen at  $6 M_{\odot}$ .

### 3. RESULTS

Accretion flow dynamics of a transient BHC can be well understood by model analysis of spectral and temporal behaviors of the source during its outburst phase. Here, we present results of spectral analysis based on TCAF and compare with combined DBB and PL model fitted results. A combined DBB and PL model fitted spectral analysis, though fitted well throughout and in some cases better than TCAF, only give gross properties of the disk such as fluxes from different components. However, TCAF goes one step further in extracting the detailed flow parameters, such as two disk rates and shock properties. Furthermore, transitions of spectral states are more conspicuous in terms of the fitted parameters. Thus, to study accretion dynamics around BHCs, there appears to be certain definite advantages in fitting with TCAF solution. A shortcoming of TCAF fit with the current version (v0.1) is that as the spectra become softer, the fit tends to worsen, mainly indicating that the importance of the halo component is reducing. In our next version this would be taken care of by self-consistently cooling down the second component in order that the flow automatically tends to have a single component.

All 30 observational IDs spreaded over the entire period of the 2010 outburst are initially fitted with combined DBB and PL model components in XSPEC. Model fitted disk temperature ( $T_{in}$  in keV), power-law photon index ( $\Gamma$ ), and flux contributions from two types of model components are obtained. We then refitted all the spectra with the current version of our TCAF model and from the fit, accretion flow parameters, such as disk rate ( $\dot{m}_d$ ), halo rate ( $\dot{m}_h$ ), location of the shock ( $X_s$ ) and compression ratio ( $R$ ) are extracted.

#### 3.1. Spectral Data Fitted by TCAF Solution and by Combined DBB and PL model

A combined conventional DBB and PL model fit in 2.5 – 25 keV energy range RXTE PCA spectra provides us with a rough estimate of flux contributions originated from both thermal (from DBB) and non-thermal (from PL) processes around a BH. From this, we also get an idea about the evolution of the average temperature of the accretion disk and spectral states by monitoring variations of  $T_{in}$  and  $\Gamma$  factors. However, from the variation of the TCAF fit parameters (such as two types accretion rates,  $\dot{m}_d$  &  $\dot{m}_h$ ; shock parameters,  $X_s$  &  $R$ ; and derived physical parameters, (such as the accretion rate ratio (ARR), shock temperature  $T_{shk}$ , shock height  $h_{shk}$ , ratio between  $h_{shk}$  to  $X_s$ ), the accretion flow dynamics and geometry variation during the outburst phase become very evident. In Appendix Table I, all these fitted/derived parameters are written in a tabular form with estimated errors.

Figures 1-3 show the variation of X-ray intensities, QPO frequencies along with TCAF and combined DBB, PL model fitted and derived (from TCAF) parameters. In Fig. 1a, variation of the background subtracted RXTE PCA count rate in 2 – 25 keV (0 – 58 channels) energy band with day (MJD) is shown. In Fig. 1c, variation of TCAF fitted total accretion rates (combined Keplerian disk and sub-Keplerian halo rates) in the 2.5 – 25 keV energy band are shown. For comparison, combined DBB and PL model fitted total flux variation with day (MJD) is shown in Fig. 1b. We observe that the variation

of the TCAF fitted total flow rate (Fig. 1c) is different from the flux variations in Figs. 1(a-b) especially in early and late stages. In Fig. 1d, variation of *Accretion Rate Ratio* (ARR, defined to be the ratio of sub-Keplerian halo rate  $\dot{m}_h$  and Keplerian disk rate  $\dot{m}_d$ ) is plotted. Observed QPO frequencies (of only dominating primary QPOs) are shown in Fig. 1e. During the entire phase of the current outburst, only three spectral classes, such as *hard* (HS), *hard-intermediate* (HIMS), and *soft-intermediate* (SIMS) are observed. Strangely, the soft state (SS) is not prominent and possibly missing. The sequence is found to be: HIMS (rising)  $\rightarrow$  SIMS  $\rightarrow$  HIMS (declining)  $\rightarrow$  HS. We believe that the absence of HS in the rising phase is due to observational constraints. The detailed behavior of these spectral states and other reports in the literature on them are discussed in the next Section.

In Fig. 2, variation of TCAF fitted and derived shock parameters, together with combined DBB & PL model fitted results are shown. In Figs. 2(a-b), variation of DBB temperature ( $T_{in}$  in keV) and power-law photon index ( $\Gamma$ ) with day (MJD) are shown. In Figs. 2(c-d), TCAF fitted shock location ( $X_s$  in  $r_g$ ) and compression ratio ( $R$ ) are plotted with day. In Fig. 2(e-f), variation of shock height ( $h_{shk}$  in  $r_g$ ) and temperature ( $T_{shk}$  in  $10^{10}$  K, which is the initial temperature of CT95 iteration process), derived from  $X_s$  &  $R$  and using Eqs. 4 & 5 respectively of DMC15, are shown. In Fig. 2g, ratio between shock height and location are plotted. In Figs. 3(a-b), variations of DBB flux from DBB & PL model fits and Keplerian disk rate from TCAF fits with day (MJD) are compared. Similarly, in Figs. 3(c-d), variations of PL flux and sub-Keplerian halo rate from these respective models are compared. Clearly there are ‘some’ similarities in each pair of compared quantities, but not totally, since the power-law flux is a function of disk rate as well. In Figs. 4(a-c), TCAF fitted 2.5 – 25 keV background subtracted PCA spectra of three different spectral states (selected from approximate middle of each state to get better understanding, marked as a, b and c in Col. 1 of Appendix Table I) along with residual  $\chi^2$  are shown. In Fig. 4d, we show unabsorbed theoretical spectra in 0.001 – 3950 keV energy range, which are used to fit observed spectra presented in Figs. 4(a-c).

#### 3.2. Evolution of Spectral and Temporal Properties during the Outburst

Detailed temporal and spectral properties of this candidate during this outburst are discussed by several authors on the basis of X-ray variability, QPO observations, spectral results based on inbuilt XSPEC model fits, such as, power-law and multi-color DBB components, etc. (Muñoz-Darias et al. 2011; Kalamkar et al. 2011, etc.). However, since TCAF provides us with variation of physical parameters from the spectral fits on a daily basis, it may be possible find a pattern to correlate with spectral classes. We found interesting correlation in 2010 outburst of H 1743-322 (MDC14) and in 2010-11 outburst of GX 339-4 (DMC15). In Figs. 1d and 1e, we see variations of ARR and QPO frequencies with time in MJD. We find that ARR, total flow/accretion rate ( $\dot{m}_d + \dot{m}_h$ ), shock locations, compression ratios, etc. in conjunction with QPOs provide a better understanding on the classification of spectral states. This will be discussed below.

(i) *Hard-Intermediate State in the Rising phase*: RXTE has started observing the source three days after its discovery. Probably the initial low-hard state of the source in the rising phase was missed. For the first 3 days of our obser-

vation (from MJD = 55467.19 to 55469.09), source was in a hard-intermediate state with increasing thermal DBB flux (also, Keplerian disk rate; see, Figs. 1 & 3). From Fig. 3d, it is seen that during this phase, TCAF fitted sub-Keplerian halo rate shows a rapid fall, although combined DBB & PL model fitted non-thermal PL flux is not changed significantly. This fact can be better understood by observing variations of ARR in Fig. 1d. The shock moved rapidly (from  $\sim 354$  to  $207 r_g$ ) towards the black hole with reducing shock strength and height. This third observed day (2010 Sept. 30, MJD = 55469.09) is the transition day from hard-intermediate to soft-intermediate spectral states. QPO frequency increased monotonically (from 1.607 Hz to 2.723 Hz) with time (day) and ARR values decreased rapidly (from 3.259 to 0.590). According to propagating oscillatory shock (POS) model (Chakrabarti et al. 2005, 2008, 2009; Debnath et al. 2010, 2013; used to explain monotonic evolutions of QPO frequencies during rising and declining phases of the outburst), QPO rises rapidly till the compression ratio  $R$  reaches nearly around unity as the post-shock is cooled down. This is also seen in this outburst as well (Fig. 2d).

(iii) *Soft-Intermediate State:*

The constancy of ARR lasted till the total rate as well as non-thermal (PL) flux or halo rate started rising suddenly on 2010 Nov. 01 (MJD = 55501.23). This phase continued for  $\sim 32$  days, where sporadic QPOs are observed with very little changes in ARR,  $T_{in}$ ,  $\Gamma$ ,  $R$ ,  $T_{shk}$ ,  $h_{shk}$ , and  $X_s$  are observed. During this phase, the total X-ray intensity, flux or flow rate initially increased and then decreased mainly because of similar variations in thermal DBB flux or Keplerian disk rate. In this phase of the outburst, non-thermal PL flux shows decreasing pattern, although sub-Keplerian halo rate initially decreases, and then becomes more or less constant. On the soft-intermediate to declining hard-intermediate transition day, a rise in ARR value due to the effect of sudden rise in non-thermal PL flux/halo rate is observed. On this day, QPO frequency had a maximum (5.951 Hz).

(vi) *Hard-Intermediate State in the Declining phase:* This state continued for the next  $\sim 3$  days, starting from the SIMS-HIMS (declining) transition day. During this phase QPO frequency decreases rapidly from 5.951 Hz to 2.563 Hz. ARR is found to increase slowly with a rise in halo rate compared to the disk rate (see, Figs. 1 & 3). Rapid decrease in power-law photon-index ( $\Gamma$ ) also indicates that spectrum start to become harder from the day one of this state. A slow movement of the receding shock with little increment in the compression ratios and shock heights are observed during this phase of the outburst. Nov. 05, 2010 (MJD = 55504.06) is the transition day from declining hard-intermediate to hard state. Interestingly, on this day, ARR is locally maximum (=0.327) and QPO frequency starts to decrease slowly after that. Precisely this behavior was seen in our earlier TCAF fits on other BHCs (see, MDC14, DCM15) as well.

(vii) *Hard State in the Declining phase:*

The source is observed in this spectral state till the end of the observation of 2010 outburst starting from the transition day. In this state, ARR (from 0.327 to 0.278) as well as observed QPO frequencies (from 2.563 Hz to 1.638 Hz) decrease monotonically as in other objects fitted by TCAF. A slow decrease in PCA count rate, total (DBB+PL) fluxes and total flow (disk+halo) rates are observed with a similar decreasing trend in both thermal (DBB and  $\dot{m}_d$ ) and non-thermal (PL or  $\dot{m}_h$ ) flux/rate components. This is because the supply rate is dwindling after the peak outburst is over (see, Figs. 1

& 3). A fast receding shock (from  $\sim 103$  to  $416 r_g$ ) with rise in compression ratio and shock height are observed. At the same time, during this phase of the outburst, a decrease in power-law photon index is observed, which indicates that the spectrum becomes harder with a clear dominance by the sub-Keplerian halo and non-thermal power-law photons. Shock temperature ( $T_{shk}$  of initial iteration) values are found to decrease monotonically with time (day).

#### 4. DISCUSSIONS AND CONCLUDING REMARKS

We study the evolution of spectral properties of Galactic transient black hole candidate MAXI J1659-152 during its first (2010) X-ray outburst using the current version v0.1 of two component advective flow (TCAF) solution based model after its inclusion as a local additive table model in HEASARC's spectral analysis software package XSPEC (DCM14). This has been done with a model *fits* file using  $\sim 4 \times 10^5$  theoretical spectra which are generated by varying five model input parameters (two types of accretion i.e., Keplerian disk  $\dot{m}_d$ , sub-Keplerian halo  $\dot{m}_h$  rates; two types of shock parameters: location  $X_s$  and compression ratio  $R$ ; and the mass of the black hole  $M_{BH}$ ) to the modified CT95 code (see, DMC15 for details). We re-fitted all these spectra of MAXI J1659-152 with combined DBB and PL model components to get a rough estimate about the variations of the thermal (DBB) and non-thermal (PL) fluxes during the outburst and compare these with our TCAF fitted results (see, Figs. 1-3). In Appendix Table I, detailed results of our spectral fit with observed QPO frequencies are presented.

The entire period of the 2010 outburst of MAXI J1659-152 appears to have three spectral classes: *hard*, *hard-intermediate*, and *soft-intermediate*. It did not reach the soft state. When we study variations of TCAF parameters in these states, we find that there is a pattern in how the rates, ARR, QPO frequency etc. behave. These behaviours are similar to what were reported in other sources, (see, MDC14, DMC15). Specifically, we see a local maximum of ARR during the transition between hard-intermediate to hard states in all these sources. Clearly more objects need to be fitted before any firm conclusion can be drawn.

It is interesting that unlike other sources (MDC14, DMC15), this object exhibited no soft-states during this outburst according to our model. Only for two days, MJD=55481.71 and MJD=55485.16 the fluxes are higher (Table I of Appendix), but observation of LFQPOs and the presence of a dip on MJD=55483.92 in between, suggests that the state is not soft, but soft-intermediate. van der Horst et al. (2013), using a disk irradiation model called DISKIR (with number of free parameters significantly higher than TCAF with irradiation from CENBOL on the Keplerian disk), suggests that the object might have gone to a soft state. However, the photon index (see, Fig. 5 of van der Horst et al. 2013) of those specific days showed significant error bars and thus it is uncertain if soft states were reached. It is also possible that the inclination angle might also have played a role in hardening the spectra (as discussed in another source by Motta et al. 2010 and by explicit Monte-Carlo simulation by Ghosh et al., 2011).

Although low frequency ( $\sim 0.01 - 30$  Hz) QPOs are observed almost three decades ago, there is a debate on the origin of this temporal behavior in Fourier transformed power-density spectrum of the X-ray intensity variation. According to shock oscillation model (SOM) of Chakrabarti and his collaborators in mid-90s, it can occur when Compton cool-

ing time scale roughly agrees with infall time scale (Molteni, Sponholtz & Chakrabarti, 1996) or due to non-satisfaction of Rankine-Hugoniot conditions to form a stable shock (Ryu, Chakrabarti & Molteni, 1997). Recent numerical simulations of Garain et al. (2014) also demonstrated this in presence of Comptonization. According to SOM, the QPO frequency is inversely proportional to the infall time ( $t_{infall}$ ) in the post-shock region. It also has been observed that these QPO frequencies show monotonically increasing (during rising phase of the outburst) or decreasing (during declining phase of the outburst) nature in hard and hard-intermediate spectral states. This evolution of the QPO frequencies can be well fitted with the POS model, which is nothing but time varying form of the SOM. Movement of the shock inward could be due to rapid cooling and consequent collapse of the CENBOL (in the rising phase) and outward, due to the lack of cooling in the declining phase (Mondal, Chakrabarti & Debnath, 2015).

In soft-intermediate spectral states, sporadic QPOs are observed, which may be due to appearance or disappearance of the oscillating component, namely, CENBOL by intrusion of strong toroidal magnetic fields. Strong sporadic jets are also seen in these states (e.g., Nandi, et al. 2001; Radhika & Nandi 2014). Our current TCAF model takes care of the combined effects of CENBOL and the outflow. Separation of the effects of CENBOL and jets is possible from more detailed modeling of timing properties and will be incorporated in a later version of TCAF.

Recently, it has been shown (DMC15, MDC14) using examples of 2010-11 outburst of Galactic BHC GX 339-4 and 2010 outburst of Galactic BHC H 1743-322 how spectral state transitions may be triggered when the relative ratio of the ac-

cretion rates, namely, ARR, vary in specific ways. The nature of variation of QPOs (when observed), shock locations, strengths etc. are also very specifically. Exactly same type of variation of the fitted parameters are also seen for the current source MAXI J1659-152. From the observed variation of Keplerian rates in these objects, we believe that an outburst is triggered due to a sudden rise in viscosity and is turned off due to the reduction in viscosity (CT95, Ebisawa, et al. 1996; Chakrabarti, Dutta & Pal, 2009). It is possible that this object belongs to a category, with short orbital period, where accretion disk around the black hole is mostly dominated by the wind accretion compared to disk accretion. The Keplerian disk is always immersed inside a strong sub-Keplerian halo. So, the soft state may be difficult to achieve. In future, we will make detailed spectral and temporal study of other such objects (for e.g., XTE J1118+480 of orbital period  $\sim 4.1$  hrs, González-Hernández et al. 2013; Swift J1753.5-0127 of orbital period  $\sim 3.2$  hrs, Zurita et al. 2007) during their X-ray outbursts to check if flow dynamics of these sources also follow a similar trend. Prediction of QPO frequency from TCAF solution fitted shock parameters ( $X_s$  &  $R$ ; DCM14), and comparative study with POS model solution will be published elsewhere.

#### ACKNOWLEDGMENTS

A. A. Molla acknowledges supports of DST sponsored Fast-track Young Scientist project fellowship and MoES sponsored Junior Research Fellowship. Mr. S. Mondal acknowledges the support of CSIR-NET scholarship. DD acknowledges supports from project funds of DST sponsored Fast-track Young Scientist and ISRO sponsored RESPOND.

#### REFERENCES

- Belloni, T., Homan, J., Casella, P., et al., 2005, *A&A*, 440, 207  
 Chakrabarti, S. K., 1990a, "Theory of Transonic Astrophysical Flows", World Scientific (Singapore) (C90a)  
 Chakrabarti, S. K., 1990b, *ApJ*, 362, 406 (C90b)  
 Chakrabarti, S.K., & Titarchuk, L.G., 1995, *ApJ*, 455, 623 (CT95)  
 Chakrabarti, S. K., 1996, *ApJ*, 464, 66d4  
 Chakrabarti, S.K., 1997, *ApJ*, 484, 313 (C97)  
 Chakrabarti, S. K., Nandi, A., & Debnath, D., et al., 2005, *IJP*, 79, 841 (arXiv:astro-ph/0508024)  
 Chakrabarti, S.K., Debnath, D., & Nandi, A., et al., 2008, *A&A*, 489, L41  
 Chakrabarti, S.K., Dutta, B.G. & Pal, P.S., 2009, *MNRAS*, 394, 1463  
 Debnath, D., Chakrabarti, S.K., & Nandi, A., et al., 2008, *BASI*, 36, 151  
 Debnath, D., Chakrabarti, S.K., & Nandi, A., 2010, *A&A*, 520, 98  
 Debnath, D., Chakrabarti, S.K., & Nandi, A., 2013, *AdSpR*, 52, 2143  
 Debnath, D., Mondal, S., & Chakrabarti, S.K., 2014, *MNRAS*, 440, L121 (DCM14)  
 Debnath, D., Mondal, S., & Chakrabarti, S.K., 2015, *MNRAS*, 447, 1984 (DMC15)  
 Ebisawa, K., Titarchuk, L.G., & Chakrabarti, S.K., 1996, *PASJ*, 48, 59  
 Galeev, A.A., Rosner, R., & Vaiana, G.S., 1979, *ApJ*, 229, 318  
 Garain, S., Ghosh, H., & Chakrabarti, S.K., 2014, *MNRAS*, 437, 1329  
 Ghosh, H., Garain, S., Giri, K., Chakrabarti, S.K., 2011, *MNRAS*, 416, 959  
 Giri, K., & Chakrabarti, S.K., 2013, *MNRAS*, 430, 2836  
 Giri, K., Garain, S. & Chakrabarti, S.K., 2015, *MNRAS* (in press) (arXiv:1502.00455)  
 González-Hernández, J. I., Rebolo, R. & Casares, J., 2013, *hsa7.conf*, 561  
 Haardt, F., & Maraschi, L., 1993, *ApJ*, 413, 507  
 Kalamkar, M, Homan, J., & Altamirano, D., et al., 2011, *ApJ*, 731, 2  
 Keena, J. A., Krimm, H., & Mangano, V., et al., 2010, *ATel*, 2877, 1  
 Kaur, R., Kapapr, L., & Ellerbroek, L. E., et al., 2012, *ApJ*, 746, L23  
 Kuulkers, E., Ibarra, A., & Pollock, A., et al., 2010, *ATel*, 2912, 1  
 Kuulkers, E., Kouveliotou, C., & Belloni, T., et al., 2013, *A&A*, 552A, 32  
 Maccarone, T. J. & Coppi, P. S., 2003, *MNRAS*, 338, 189  
 Mandal, S. & Chakrabarti, S.K., 2010, *ApJ*, 710, L147  
 Mangano, V., Hoversten, E. A., & Markwardt, C. B., et al., 2010, *GCN*, 11296  
 McClintock, J. E., & Remillard, R. A., 2006, in *Compact Stellar X-ray Sources*, ed. W. Lewin & M. van der Klis, 39, 157  
 Miller-Jones, J. C. A., Madej, O. K., & Jonker, P. G., et al., 2011, *ATel*, 3358, 1  
 Molla, A. A., Debnath, D., & Chakrabarti, S. K., et al., 2015, *MNRAS* (In preparation, Paper II)  
 Molteni, D., Sponholz, H., & Chakrabarti, S.K., 1996, *ApJ*, 457, 805  
 Mondal, S., Chakrabarti, S.K., & Debnath, D., 2014a, *Ap&SS*, 353, 223  
 Mondal, S., Debnath, D., & Chakrabarti, S.K., 2014b, *ApJ*, 786, 4 (MDC14)  
 Mondal, S., Chakrabarti, S.K., & Debnath, D., 2015, *ApJ*, 798, 57  
 Motta, S., Muñoz-Darias, T. & Belloni, T., 2010, *MNRAS* 408, 1796  
 Muchotrzeb, B & Paczyński, B., 1982, *Acta Astron.*, 32, 1  
 Muñoz-Darias, T., Motta, S., & Stiele, et al., 2011, *MNRAS*, 415, 292  
 Nandi, A., Chakrabarti, S. K., & Vadawale, S. V. et al., 2001, *A&A*, 380, 245  
 Nandi, A., Debnath, D., Mandal, S., & Chakrabarti, S.K., 2012, *A&A*, 542, 56  
 Negoro, H., Yamaoka, K., & Nakahira, S., et al., 2010, *ATel*, 2873, 1  
 Novikov, I., & Thorne, K.S., 1973, in *Black Holes*, Ed. C. DeWitt & B.S. DeWitt (New York: Gordon & Breach), 343  
 Okuda, T., Teresi, V. & Molteni, D., 2007, *MNRAS* 377, 1431  
 Paczyński, B., & Witta, P.J., 1980, *A&A*, 88, 23  
 Paragi, Z., van der Horst, A. J., & Belloni, T., et al., 2013, *MNRAS*, 432, 1319  
 Radhika, D. & Nandi, A., 2014, *AdSpR*, 54, 1678  
 Remillard, R.A., & McClintock, J.E., 2006, *ARA&A*, 44, 49  
 Russel, D. M., Lewis, F., & Bersier, D., et al., 2010, *ATel*, 2884, 1  
 Ryu, D., Chakrabarti, S.K., & Molteni, D., 1997, *ApJ*, 474, 378  
 Shakura, N.I., & Sunyaev, R.A., 1973, *A&A*, 24, 337 (SS73)  
 Shaposhnikov, N., Swank, J.H., & Markwardt, C., et al., 2011 (arXiv:1103.0531)  
 Sunyaev, R.A., & Titarchuk, L.G., 1980, *ApJ*, 86, 121  
 Sunyaev, R.A., & Titarchuk, L.G., 1985, *A&A*, 143, 374  
 van der Horst, A.J., Curran, P.A., & Miller-Jones, J.C.A., et al., *MNRAS*, 436, 2625  
 Yamaoka, K., Allured, R., & Kaaret, P, et al., 2012, *PASJ*, 64, 32

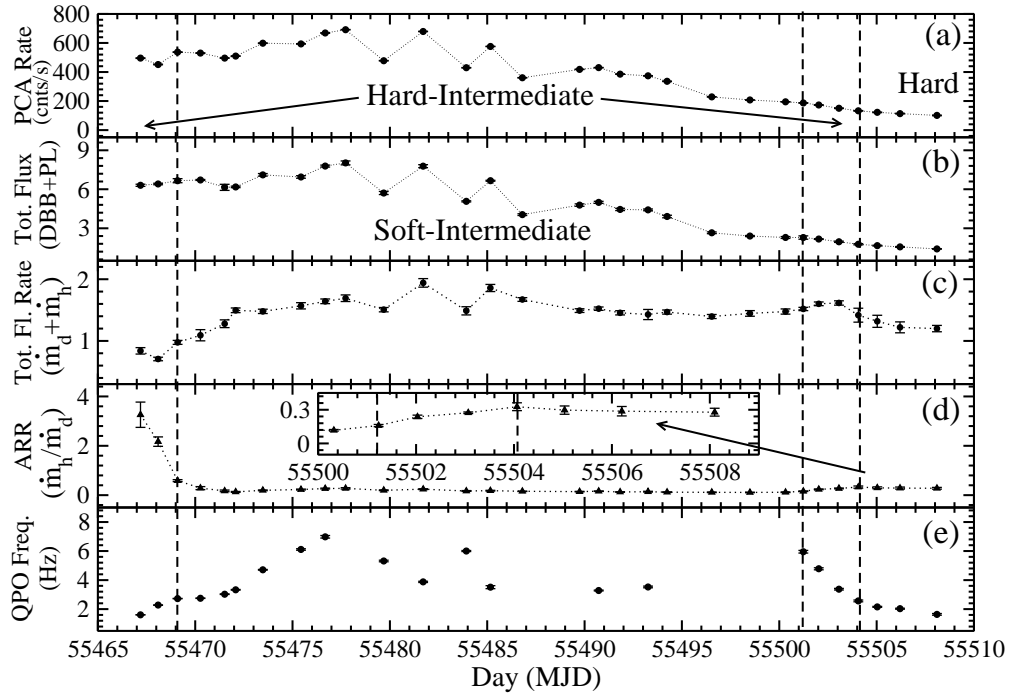


FIG. 1.— Variation of (a) 2 – 25 keV PCA count rates (cnts/sec), (b) combined disk black body (DBB) and power-law (PL) model fitted total spectral flux in 2.5 – 25 keV range (in units of  $10^{-9} \text{ ergs cm}^{-2} \text{ s}^{-1}$ ), (c) TCAF model fitted total flow (accretion) rate (in  $M_{Edd}$ ; sum of Keplerian disk,  $\dot{m}_d$  and sub-Keplerian halo  $\dot{m}_h$  rates) in the 2.5 – 25 keV energy band, and (d) Accretion Rate Ratio (ARR; ratio between halo and disk rates) with day (MJD) for the 2010 outburst of MAXI J1659-152 are shown. In the bottom panel (e), observed primary dominating QPO frequencies (in Hz) with day (MJD) are shown. The vertical dashed lines indicate the transitions of between different spectral states.

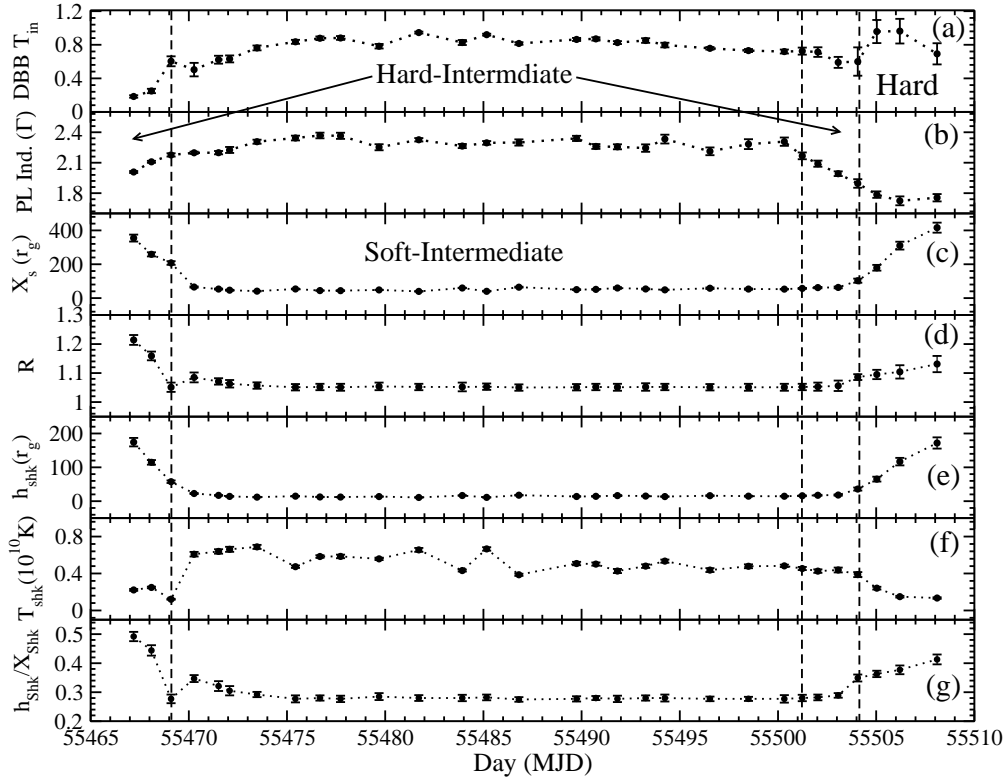


FIG. 2.— Variation of combined DBB and PL model fitted (a) disk temperature  $T_{in}$  (in keV), and (b) PL photon index ( $\Gamma$ ) with day (MJD) are shown in top two panels. Variation of TCAF model fitted/derived shock (c) location ( $X_s$  in  $r_g$ ), (d) compression ratio ( $R$ ), (e) temperature ( $T_{shk}$  in  $10^{10}$  K), (f) height ( $h_{shk}$  in  $r_g$ ), and (g) ratio between  $h_{shk}$  &  $X_s$ , with day (MJD) are shown. The shock height, and temperature are derived from Eqs. 4 & 5 respectively of DMC15.

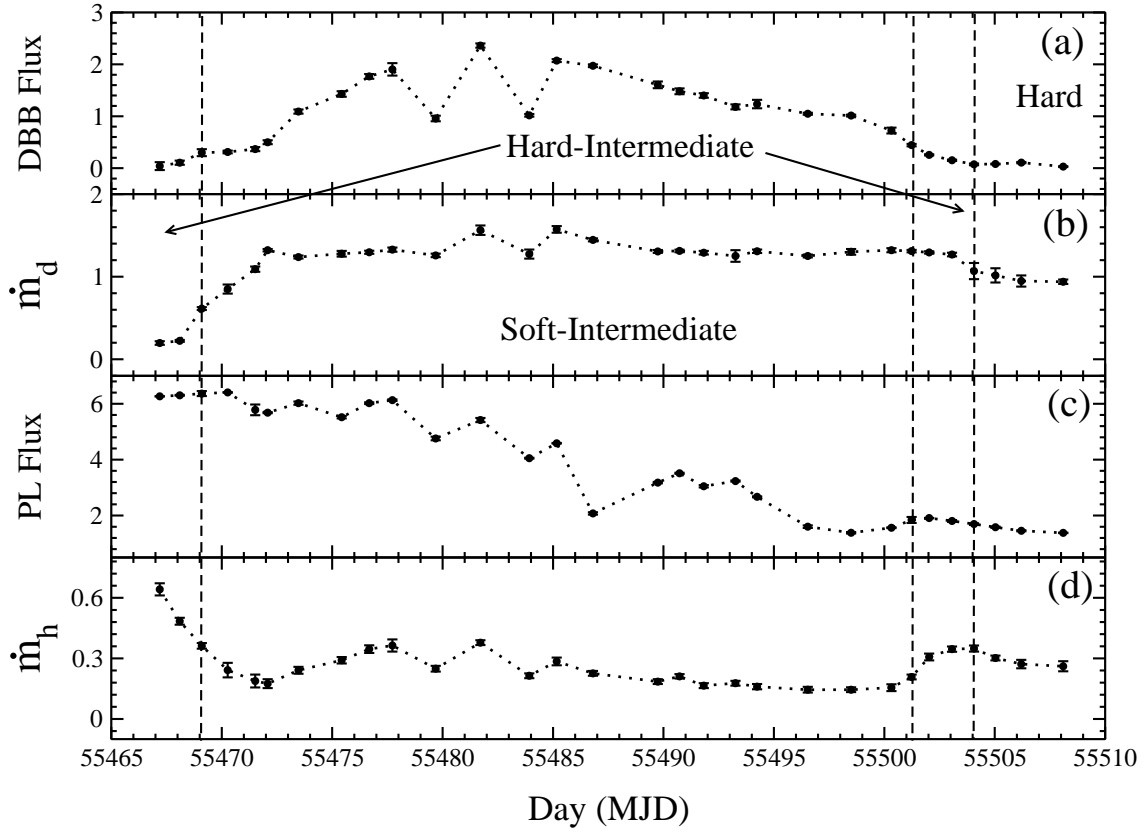


FIG. 3.— In top panel (a), the variation of combined disk black body (DBB) and power-law (PL) model fitted DBB spectral flux and in panel (c), the variation of PL spectral flux (both in units of  $10^{-9} \text{ ergs cm}^{-2} \text{ s}^{-1}$ ) in 2.5 – 25 keV energy range are shown. In panel (b), the variation of TCAF model fitted Keplerian disk rate  $\dot{m}_d$  and in bottom panel (d), the variation of sub-Keplerian halo rate  $\dot{m}_h$  (both in  $M_{Edd}$ ) in the same energy band are shown.

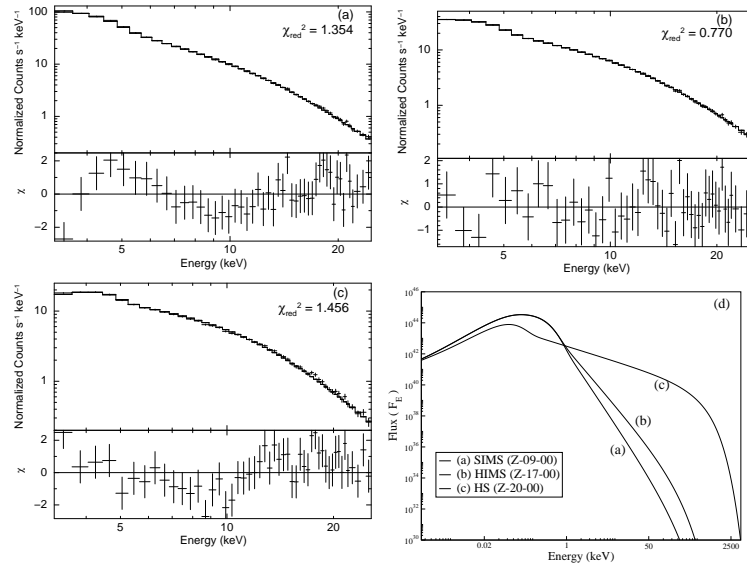


FIG. 4.— TCAF model fitted 2.5 – 25 keV PCA spectral flux, in units of  $NormalizedCounts \text{ s}^{-1} \text{ keV}^{-1}$  with variation of  $\Delta\chi$ , selected from three different spectral states: soft-intermediate, hard-intermediate, and hard states respectively are shown in plots (a-c). The observation IDs (where Z=95118-01) and fitted values of  $\chi^2_{red}$  are written down in the plots. In bottom-right plot (d), unabsorbed TCAF model generated spectra, which are used to fit these spectra are shown.

